

THE SOLUTION CONFORMATION OF NOVEL ANTIBODY FRAGMENTS STUDIED USING THE OPTIMA™ XL-A ANALYTICAL ULTRACENTRIFUGE

Peter J. Morgan, Olwyn D. Byron, Stephen E. Harding
Department of Applied Biochemistry and Food Science, University of Nottingham,
Sutton Bonington, U.K.

INTRODUCTION

One of the latest attempts to improve monoclonal antibodies in their use as radiolabeled diagnostic markers (1) has involved the cross-linking of novel Fab' fragments. It is expected that a relationship exists between the spacing of the antigen binding sites at the extremes of the Fab' fragments in solution and their immunological performance in vitro and in vivo.

In order to properly understand the function of these new antibody fragments *in vivo*, it is critical to have an appreciation of their size, self-association behavior (or preferably lack of) and solution conformation. Appropriate application of the Optima™ XL-A analytical ultracentrifuge can provide this data. No other single technique provides this breadth of information.

The flexibility conferred upon the cross-linked $F(ab')_2$ by its linker precludes the determination of its conformation via protein x-ray crystallography. However, the sedimentation coefficients of both the $F(ab')_2$ and Fab' fragments when combined with radius of gyration data obtained from small angle x-ray scattering experiments provide a useful gauge of solution conformation.

In this study the monodispersity and absence of self-association phenomena of Fab' and $F(ab')_2$ solutions are strongly indicated by sedimentation velocity and sedimentation equilibrium experiments. The weight average molecular weights measured are shown to be in complete agreement with the molecular weights as calculated from amino acid sequences. Finally, sedimentation coefficients have been measured, and we indicate how these can be used to access conformation when combined with other solution measurements.

METHODS

The Fab' and $(Fab')_2$ fragments (kindly supplied by Celltech Ltd.) were dissolved in a standard phosphate chloride buffer ($I = 0.1$, $pH = 6.8$). The Beckman Optima XL-A analytical ultracentrifuge was employed to perform both sedimentation velocity and sedimentation equilibrium experiments. Solute distributions at $20.0^\circ C$ were recorded via their absorption at 278 nm.

Sedimentation Velocity

Consecutive scans were recorded at regular intervals, utilizing the "autoscan" facility. Sedimentation coefficient ($s_{20,w}$) values were deter-

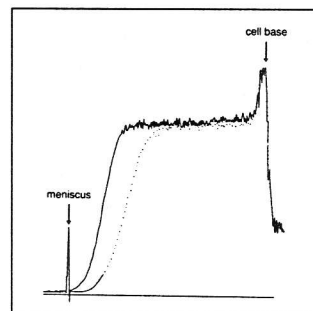


Figure 1a. Sedimentation velocity profiles for Fab' . Loading concentration = 2.0 mg/ml; rotor speed = 49,000 rpm; scan interval = 27 min. The direction of sedimentation is from left to right.

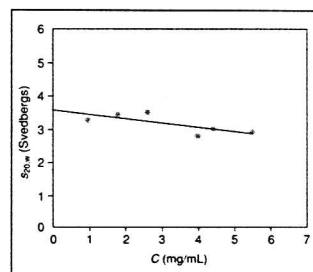


Figure 1b. Plot of sedimentation coefficient versus concentration for Fab' . Run conditions were as above.

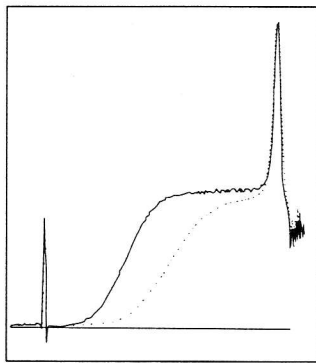


Figure 2a. Sedimentation velocity profiles for $F(ab')_2$. Loading concentration = 6.6 mg/mL; rotor speed = 49,000 rpm; scan interval = 18 min. The direction of sedimentation is from left to right.

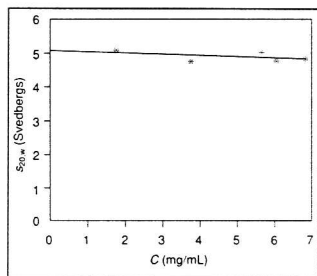


Figure 2b. Plot of sedimentation coefficient versus concentration for $F(ab')_2$. Run conditions were as above.

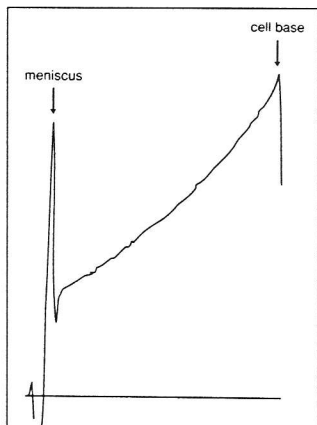


Figure 3a. Sedimentation equilibrium of Fab' . Solute distribution recorded at 9000 rpm. Loading concentration = 0.5 mg/mL.

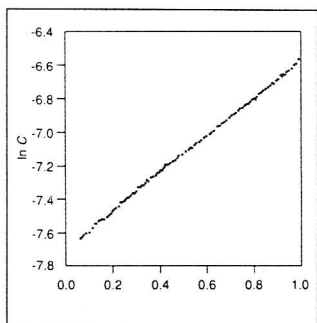


Figure 3b. Plot of $\log(\text{absorbance})$ versus ξ for Fab' .

mined in the standard way and plotted against concentration (corrected for radial dilution). Extrapolation to infinite dilution yielded $s'_{20,w}$.

Sedimentation Equilibrium

The low-speed sedimentation equilibrium method was employed. The low-speed method is more accurate since it provides more data points over the entire radial pathlength compared with the high-speed sedimentation equilibrium method (see e.g., Ref. 2.) It was considered that equilibrium had been established when two consecutive scans, recorded several hours apart, appeared identical. Multichannel (Yphantis type (3)) centerpieces were employed to permit the simultaneous measurement of multiple samples. The final solute distribution ASCII data were captured and analyzed on the IBM 3084Q Phoenix mainframe at the University of Cambridge, using the FORTRAN MSTAR program (4). Whole-cell weight average molecular weights (M_w^0) were extracted by using the limiting value at the cell base of the M^* (point average molecular weight) function (2). (An independent estimate for the initial loading concentration was not required.) Partial specific volumes were calculated from the amino acid sequence for the fragments (see e.g., Ref. 5).

RESULTS AND DISCUSSION

Confirmation of Monodispersity and Absence of Self-Association Phenomena

This was supported by (i) the observation of only single boundaries from sedimentation velocity (Figures 1a and 2a), (ii) no evidence of an increase in sedimentation coefficients with increase in concentration (Figures 1b and 2b), and (iii) linear plots of $\log(\text{absorbance})$ versus distance squared (Figures 3b and 4b) from sedimentation equilibrium.

Absolute Molecular Weights

The absolute molecular weights (i.e., not requiring assumptions concerning calibration standards), M_w^0 , calculated from the limiting form of the function M^* to the cell base (see Ref. 2) were $47,000 \pm 2000$ for Fab' (Figure 3c) and $94,000 \pm 2000$ for $F(ab')_2$ (Figure 4c). These are in almost exact agreement with the polypeptide sequence molecular weights of 47,499 and 94,996, respectively. This demonstrates both the accuracy of the Optima XL-A and the homogeneity of the antibody preparations.

Sedimentation Coefficients

The $s'_{20,w}$ values for the Fab' and $F(ab')_2$ fragments were determined as 3.6 ± 0.2 S and 5.1 ± 0.2 S, respectively (Figures 1b and 2b). The relationship between these values and molecular weight are in accord with the sedimentation behavior of other globular proteins that have been well characterized.

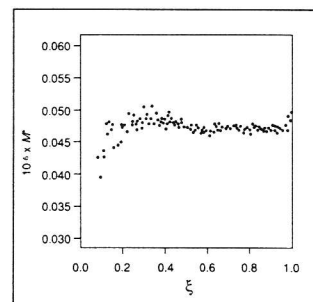


Figure 3c. Plot of M^* function versus ξ (the normalized radial displacement parameter) for Fab' . $\xi = (r^2 - a^2)/(b^2 - a^2)$ where r is the radial displacement and a and b are the corresponding values at the cell meniscus and base, respectively.

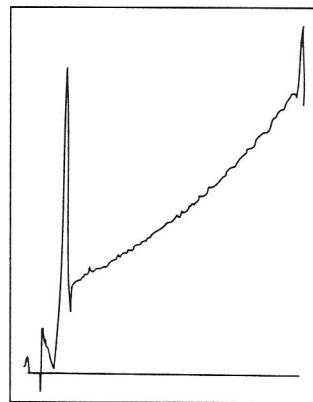


Figure 4a. Sedimentation equilibrium of $F(ab')_2$. Solute distribution recorded at 9000 rpm. Loading concentration = 0.5 mg/mL.

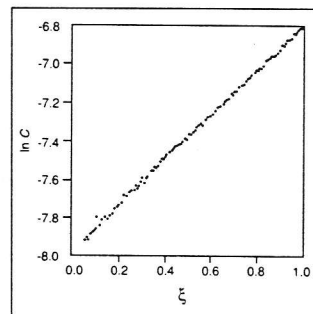


Figure 4b. Plot of $\log(\text{absorbance})$ versus ξ for $F(ab')_2$.

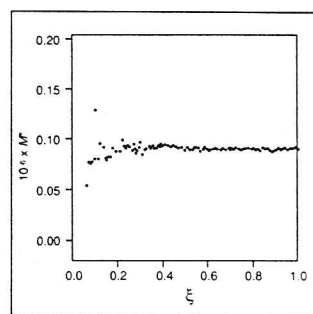


Figure 4c. Plot of M^* function versus ξ (the normalized radial displacement parameter) for $F(ab')_2$.

Solution conformation modeling

The $s_{20,w}^0$ values so found can be used as a useful handle on the conformation of these molecules in solution. Using simple formulae (6), a combination of the $s_{20,w}^0$ and molecular weight data yields estimates for the frictional ratios (f/f_0) of 1.31 ± 0.11 and 1.47 ± 0.08 , respectively. These values can be interpreted in terms of simple ellipsoid models (see Ref. 7), or, more usefully, it is possible to use this data to model conformation in terms of sophisticated hydrodynamic bead models using the FORTRAN program TRV (8). However, this increased sophistication requires additional data from other solution measurements, such as x-ray scattering. For example, the hydrodynamic bead model shown in Figure 5 for Fab' was constructed on the basis of an initial estimate for the solution conformation based on static x-ray crystallographic coordinates (9) for the Fab' fragment of monoclonal antibody R19.9 and subsequently modified in order to reproduce f/f_0 (or equivalently $s_{20,w}^0$) and a radius of gyration of $26 \pm 3 \text{ \AA}$ obtained from small angle x-ray scattering experiments. These data are currently being extended by us to model the conformation of $F(ab')_2$, particularly in terms of antigen binding site separation, with the ultimate aim of adequately representing the solution conformation of the intact parent antibody.

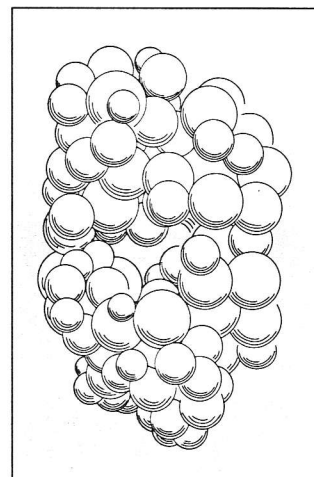


Figure 5. Hydrodynamic bead model for Fab' of chimeric B72.3 (Celltech Ltd), based on sedimentation coefficient and radius of gyration data. The sphere coordinates and radii were generally such that their maximum diameter is 10 \AA . The overall dimensions of this model are approximately $50 \times 80 \times 50 \text{ \AA}$, inclusive of hydration.

REFERENCES

1. Begent, R. H. J. Recent advances in tumour imaging. Use of radiolabeled antitumour antibodies. *Biochim. Biophys. Acta* 780, 151-166 (1985)
2. Creeth, J. M., Harding, S. E. Some observations on a new type of point average molecular weight. *J. Biochem. Biophys. Methods* 7, 25-34 (1982)
3. Yphantis, D. A. Equilibrium ultracentrifugation of dilute solutions. *Biochemistry* 3, 297-317 (1964)
4. Harding, S. E., Horton, J. C., Morgan, P. J. MSTAR: a FORTRAN program for the model independent molecular weight analysis of macromolecules using low or high speed sedimentation equilibrium. *Analytical Ultracentrifugation in Biochemistry and Polymer Science, Chapter 15*. Edited by S. E. Harding, J. C. Horton and A. J. Rowe. Cambridge, Royal Society of Chemistry, (in press).
5. Perkins, S. J. Protein volumes and hydration effects. The calculations of partial specific volumes, neutron scattering matchpoints and 280-nm absorption coefficients for proteins and glycoproteins from amino acid sequences. *Eur. J. Biochem.* 157, 169-180 (1986)
6. van Holde, K. E. Sedimentation. *Physical Biochemistry*, pp. 110-121. 2nd ed. Englewood Cliffs, N. J., Prentice Hall, 1985.
7. Harding, S. E. Modelling the gross conformation of assemblies using hydrodynamics: the whole body approach. *Dynamic Properties of Biomolecular Assemblies*, pp. 32-56. Edited by S. E. Harding and A. J. Rowe. Cambridge, Royal Society of Chemistry, 1989.
8. de la Torre, J. G. Hydrodynamic properties of macromolecular assemblies. *Dynamic Properties of Biomolecular Assemblies*, pp. 3-31. Edited by S. E. Harding and A. J. Rowe. Cambridge, Royal Society of Chemistry, 1989.
9. Lascombe, M. B., Alzari, P. M., Boulot, G., Saludjian, P., Tougaard, P., Berek, C., Haba, S., Rosen, E. M., Nisonoff, A., Poljak, R. J. Three-dimensional structure of Fab R19.9, a monoclonal murine antibody specific for the p-azobenzene arsonate group. *Proc. Natl. Acad. Sci.* 86, 607-611 (1989)